Laser Rastering Flow Cytometry: Fast Cell Counting and Identification

G. Vacca, M. R. Junnarkar, N. R. Goldblatt, M. W. Yee, B. M. Van Slyke, T. C. Briese
in *Proceedings of SPIE* **7182**, 71821T (2009).

Contact:
Giacomo Vacca, Ph.D.
(650) 269-0726
GVacca@KineticRiver.com
www.linkedin.com/in/GVacca
www.KineticRiver.com

KINETIC RIVER™
Advancing ideas.™

Laser rastering flow cytometry: fast cell counting and identification

G. Vacca[a]*, M. R. Junnarkar[a], N. R. Goldblatt[a], M. W. Yee[a], B. M. Van Slyke[b†], T. C. Briese[b]
[a]Abbott Hematology, 5440 Patrick Henry Drive, Santa Clara, CA USA 95054
[b]Plexus Technology Group, 361 Centennial Drive, Suite 300, Louisville, CO USA 80027

ABSTRACT

We describe the concept of laser rastering flow cytometry, where a rapidly scanning laser beam allows counting and classification of cells at much higher rates than currently possible. Modifications to existing flow cytometers to implement the concept include an acousto-optic deflector, fast analog-to-digital conversion, and a two-step digital-signal-processing scheme that handles the high data rates and provides key assay information. Results are shown that prove the concept, demonstrating the ability to resolve closely spaced cells and to measure cells at rates more than an order of magnitude faster than on conventional flow-cytometer-based hematology analyzers.

Keywords: flow cytometry, hematology, light scattering, fluorescence, acousto-optic deflector, digital signal processing

1. INTRODUCTION

Flow cytometers and their close relatives, automated hematology analyzers, are remarkable instruments that draw on the strength of several disparate disciplines to perform their main function (cell-based assays): biochemistry, fluid dynamics, optics, and electronics, to name the key ones. Stripped down to the bare bones, a flow cytometer aspirates a sample, incubates it with one or more reagents, and pipes the resulting solution to a flowcell, where the cells in the sample interact individually with a tightly focused laser beam; the signals produced by the interaction (consisting of scattered and sometimes also fluorescently emitted light) are collected, electronically preprocessed, and then further analyzed by algorithms in order to count, identify, and classify the measured cells.

As an example of the sophistication and complexity that have been built into these kinds of machines, consider the onboard reagent chemistry. Commercial requirements for high-end hematology analyzers dictate that the result of most assays be available within less than a minute from the moment blood is aspirated from the sample tube; this in turn places hard time constraints on the reagent kinetics and on incubation. Among the functions the reagents are required to perform are: sphering of the natively biconcave red blood cells (RBCs) to reduce orientation dependence of the scattering signals; staining of nuclear material with dyes; surface-antigen binding to fluorescently conjugated monoclonal antibodies; and (in some assays) lysis of the vastly more numerous RBCs to allow counting and identification of white blood cells (WBCs). Add to all this the expectation that the instrument deliver accurate results for all blood types, irrespectively of patient age, gender, ethnicity, and pathology (all of which can affect greatly the hematological profile), and the challenges even just for managing reagent performance become evident.

The complexities only multiply in those areas where several subsystems interact, as is the case for the flowcell. Here the sample-reagent solution undergoes the process known in the field as hydrodynamic focusing, where the sample stream and a sheath solution emerge from concentric nozzles (the sample in the inside flow stream) and jointly enter a conical region where the fluids accelerate dramatically while squeezing into a capillary. This results in a thinning of the sample stream from roughly 1 mm to barely greater than a cell width (a few microns) and in center flow speeds on the order of 10 m/s. This arrangement, given proper engineering design, allows for single-cell analysis, as the cells in the dilute suspension fly rapidly in single file past the point of interrogation—the focus of the laser beam. Stability is paramount: in the rates at which fluids are piped through the flowcell, in the streamlines, in the laser beam power and angular pointing, and in the detector electronics. Needless to say, the sample should also not be appreciably altered by action of the residual reagents for the entire duration of the measurement.

* To whom correspondence should be addressed. GVacca@KineticRiver.com; tel. (650) 269-0726
* Presently at Kinetic River, 661 S. Baywood Ave., San Jose, CA USA 95128
† Presently at Covidien, Respiratory and Monitoring Solutions, 6135 Gunbarrel Avenue, Boulder, CO USA 80301

Imaging, Manipulation, and Analysis of Biomolecules, Cells, and Tissues VII, edited by Daniel L. Farkas, Dan V. Nicolau, Robert C. Leif, Proc. of SPIE Vol. 7182, 71821T · © 2009 SPIE · CCC code: 1605-7422/09/$18 · doi: 10.1117/12.820799

Given the twin sets of commercial requirements and technical constraints, flow cytometry as a field has matured to deliver a well-established set of time-tested designs. Progressive optimization of the technology, as in any field, has resulted in two sides of the same coin: dependability on one hand, and diminishing returns on the other. One area where this is especially evident is throughput—or, more specifically, the rate at which cells are measured. The success of hydrodynamic focusing has meant that most advanced designs take advantage of it, but also end up looking a lot like each other, and having similar performance tradeoffs. Turbulence considerations prevent flowing a sample stream in the capillary flowcell (with each cross-sectional dimension around 200 μm) beyond about 10 m/s. At the same time, the requirement for cell-by-cell analysis prevents concentrating the cells in the sample to the point where two of them would interact with the laser at the same time (this is called a "coincidence" and leads to undercounting).

The concept we have introduced[1] and demonstrated[2][3][4] bypasses these performance bottlenecks to yield a vastly increased measurement rate without sacrificing performance. It comes with a relatively manageable price to pay in terms of additional optics and in terms of signal processing complexity. We have termed this concept laser rastering flow cytometry.

2. CONCEPT

The essential elements of laser rastering (LR) can be best understood by comparing the design of a LR flow cytometer with that of a conventional flow cytometer.

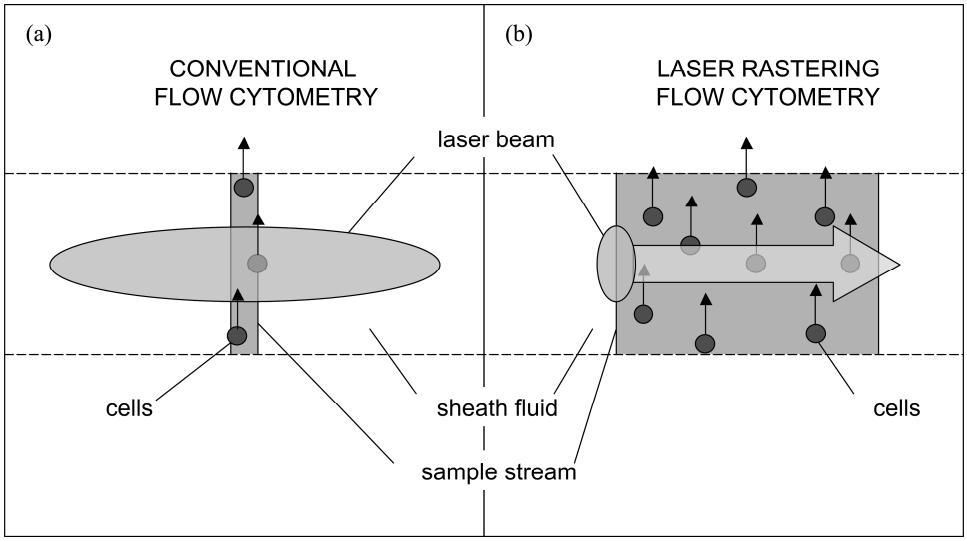

Fig. 1. The interaction region of a flowcell where cells in the flowing sample stream are interrogated by the focused laser beam spot. The flowcell walls are not shown. (a) Conventional flow cytometry: the hydrodynamically focused, narrow sample stream intersects the stationary laser beam, resulting in individual cell-by-cell interactions captured by the detectors. (b) Laser rastering flow cytometry: the still hydrodynamically focused, but much wider sample stream is rapidly and repeatedly scanned side-to-side by the tightly focused laser beam, resulting in multiple interactions with each cell.

In Fig. 1 we show, side by side, schematic diagrams of the interaction between cells and the laser beam in conventional flow cytometry [Fig. 1(a)] and in LR flow cytometry [Fig. 1(b)]. The figure illustrates the key differences between the two approaches: in LR flow cytometry, the sample stream is widened considerably, allowing a much greater flux of cells; the laser beam spot is focused much more tightly, compensating for the wider sample stream and keeping the occurrence of coincident events to an acceptably low level; and the laser beam spot is repeatedly swept from side to side so as to intercept all of the cells in the sample stream. This last operation, which gives laser rastering its name in an analogy with how images are formed on cathode-ray-tube-based television screens, also requires the beam to scan over each cell multiple times, and has important consequences in terms of signal processing, which we will discuss in Subsection 2.2. In this work we will concentrate on the optics implementation and on the signal processing approach; see our upcoming works[5] for more detailed descriptions of the implications of LR for fluidic design and reagent strategy.

2.1 Optics

The main optical layout of a LR flow cytometer is similar to time-tested designs of conventional flow cytometers. Figure 2 shows in schematic form the main elements of a LR optical bench. As in conventional flow cytometry, a laser provides the stable beam for interrogation of the cells, the beam is routed toward the flowcell with mirrors (which also provide alignment functionality), the beam aspect ratio is appropriately set by anamorphic optics, and the beam is focused onto the capillary flowcell. Inserted into this path is a deflection device used to sweep the beam from side to side at high frequency. Because of the requirements for a sweep frequency in the neighborhood of 1 MHz (discussed in Subsection 2.2), the optimal choice for the deflection device is an Acousto-Optic Deflector (AOD). This solid-state component, at its core a transparent crystal, is actuated by modulating a radiofrequency signal driving a piezoelectric transducer; the resulting acoustic wave creates a transmission Bragg grating which deflects the input beam by diffraction—different driving frequencies corresponding to different deflection angles. It is very well suited for small-angle deflections such as those called for here (on the order of a few mrad), and its compactness and lack of moving parts makes it particularly attractive in terms of manufacturability and reliability. The flowcell is very similar to those used in conventional flow cytometers, and the collection and detection schemes are likewise not significantly changed.

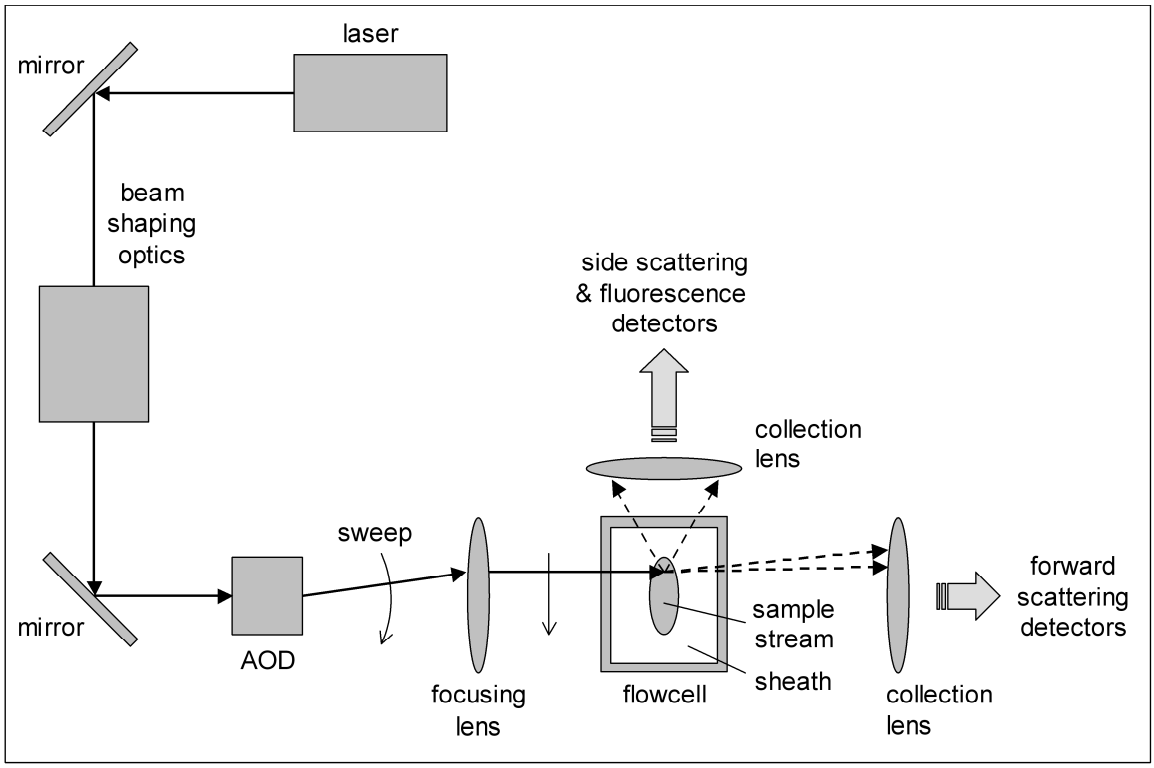

Fig. 2. Schematic layout of a LR flow cytometer optical bench. The key element, a component used to dynamically deflect the laser beam, is inserted in the optical path; an Acousto-Optic Deflector (AOD) is shown here performing this function. The rest of the layout is similar to conventional flow cytometer designs. Not to scale.

Insertion of the AOD into the optical path requires some adjustments in terms of component placement and lens strengths; the input parameters of the beam entering the AOD are dictated by the geometry of the AOD crystal and its driving configuration. In the implementation described here, care must additionally be taken in three key respects: (1) the relative positions of AOD, focusing lens, and flowcell; (2) the propagation characteristics of the output beam as it exits the crystal; and (3) the diffraction efficiency of the AOD over the range of sweep angles.

The first point is driven by the desire to avoid introducing additional complexity in the collection and detection optics. In a conventional flow cytometer, the laser beam is stationary, so the collection optical paths can be designed for a single scattering center. In LR flow cytometry, the beam is swept across the sample stream, so the location of scattering centers changes across the sweep. With a proper design, the effect of such changes can be minimized to the point where it is

negligible. One such design—a telecentric design—involves placing the AOD at the front focal plane of the focusing lens, and to place the sample stream in the flowcell at the back focal plane of the same lens. This achieves two objectives: First of all it provides the focusing necessary to convert a mildly diverging beam (as it exits the AOD) into a more tightly converging one for interaction with the cells. Second, it transforms the angular deflection imposed by the AOD into a parallel lateral translation (to a very good approximation). This second function ensures that the collection optics, designed for precise angular annuli of scattering, are insensitive to where in the sample stream the scattering light comes from—the direction of forward propagation of the incident beam being equal in all cases.

The second point (character of the output beam from the AOD) is a consequence of the geometry of the system and of the high rates of scanning. As briefly noted above, the AOD works by generating a Bragg grating in the crystal. For static applications, the acoustic wave from the transducer is fixed in frequency, and the entire beam sees the same pitch. As the radiofrequency is changed, the acoustic wave changes in pitch—the change front starting from the side of the crystal where the transducer is and traveling across the crystal. As the frequency is changed continuously ("chirped," as, e.g., in a sawtooth shape), the pitch is constantly changing and traveling across the crystal—a diffraction grating with a linearly varying pitch. The result is a cylindrical lensing effect (a "chirp lens") imposed by the AOD operation on the beam in the same plane as the angular deflection. For sufficiently high rates of frequency change, and for large enough beam widths, the lensing is noticeable. There are two consequences of this: If the lensing is strong enough that the resulting astigmatism is unacceptable, compensating optics is required. But even if the astigmatism can be lived with, the reversal of the lensing effect attendant to bidirectional scanning can result in different waist locations at the flowcell during the two scanning directions—different enough that optimization for one leads to having no detectable signals in the other. Laser rastering, then, should be carried out monodirectionally, e.g., always left to right. Because scanning always includes a return leg, even if done very quickly, what might have been a problem is in fact turned into an advantage: Since the beam on the return trip is effectively greatly defocused in the region of interest, there is no need to block it (to prevent unwanted signals) using a modulator or other means—the scattering signals are simply too weak.

The third point (diffraction efficiency of the AOD) stems from the fact that the AOD can be thought of as a dynamic transmission grating, but one where the grating pitch varies whereas the angle of incidence does not. As the driving radiofrequency changes in time and the acoustic diffraction grating pitch varies in response, the Bragg condition dictates that the grating and the incoming beam change their respective angular orientation in order to maximize diffraction efficiency. Since the incoming beam and the AOD crystal are fixed, the Bragg condition can only be satisfied at best for one angular value within the scan range, dropping off on either side. This dropoff in diffraction efficiency leads to a laser beam intensity at the flowcell that varies as a function of position. Depending on the details of AOD design, the drop from peak transmission over the desired range of several mrad can be as much as 20-25%—the worst case being at the edges if Bragg angle optimization is done near the center of the scan. There are several possible ways of countering this effect (which could severely affect the Coefficient of Variation—CV[1]—of the system). We have opted to compensate for it in the digital signal processing domain, and will comment in Subsection 2.2 below on the adopted scheme.

The collection optics and the detectors are similar to established flow cytometer designs. For example, refer to the implementation in Abbott Hematology's CELL-DYN™ analyzers, particularly the CELL-DYN Sapphire™. In that design, two photodiodes collect forward-scattering information: Axial Light Loss (ALL, a measure of beam extinction) and Intermediate Angle Scattering (IAS, the annulus from 3° to 10° of forward). On the side, three photomultiplier tubes (PMTs) collect two channels of scattering information: Polarized Side Scattering (PSS, the cone of polarization-maintaining scattered light ± 62.5° around 90° from forward) and Depolarized Side Scattering (DSS, the same as PSS but with rotated polarization), as well as up to three separate fluorescence channels: FL1 (530 ± 15 nm), FL2 (580 ± 15 nm), and FL3 (630 ± 15 nm). Sliders allow two of the PMTs to perform alternate scattering/fluorescence detection functions depending on the assay. The combination of the four scattering detection channels forms the basis of Abbott's Multi-Angle Polarized Scattering Separation (MAPSS) technology, responsible for label-free classification of the five main types of WBCs;[7] the fluorescence detection channels add capabilities such as quantification of reticulocytes (immature RBCs), detection and quantification of nucleated RBCs, and monoclonal antibody assays (e.g., quantification of CD4, the lymphocyte surface marker used in diagnosis and monitoring of AIDS).

[1] The CV of a series of measurements is defined as 100 times the standard deviation over the mean. For measurements of an ensemble of nominally identical particles (such as polymer or silica microspheres of known diameter), it provides a metric of the overall precision of the measuring apparatus and method.[6]

2.2 Signal Processing

Conventional flow cytometry signal processing essentially consists of determining the character of pulses resulting from the passage of cells through the illumination region—i.e., traversing the vertical profile of the laser beam spot intensity distribution [see Fig. 1(a)]. As the laser beam typically has a Gaussian profile (at least in the direction parallel to flow), the scattering signals are convolutions of a Gaussian with the scattering cross-section of the cell, integrated over the detection solid angle. As long as the plane-wave illumination assumption is even approximately maintained, the resulting pulse signals are, for all practical purposes, very much Gaussian in shape. The pulse height is the most common parameter extracted from the signal and used to identify cells of different types; the pulse width can also be extracted, giving complementary information regarding cell size.[2] There are several ways of converting the raw detector signals into usable numbers. Older schemes involved analog circuitry (so-called "peak-and-hold"), followed by an Analog-to-Digital Converter (ADC). Newer schemes digitize the signal waveform early on and apply various conditioning and signal processing steps in the digital domain; they are more flexible and more powerful, yet the basic function they perform (pulse height determination) is the same as in older designs.

The measurement approach introduced in LR flow cytometry is fundamentally different. There are three key differences: (1) as the laser beam is swept rapidly in a direction transversal to that of flow, the laser-cell interaction taking place in a time less than 1/10 of that typical in conventional flow cytometers (about 100 ns instead of a few μs); (2) the laser interacts with each individual cell multiple times over the course of several consecutive raster scans; (3) along any given raster scan there can be multiple cells that interact with the laser beam. While in conventional flow cytometry the signal resulting from the interaction between the laser beam and a single cell is a simple pulse, in LR flow cytometry the same interaction produces a comb of much narrower peaks, equally separated by the rastering period, and rising and falling under a broad envelope. The rate of flow in the sample stream, together with the vertical width of the laser beam and the rastering frequency, determine how many passes the beam will make over any single cell.

The reason for requiring multiple passes over a cell is that, unlike in conventional flow cytometry, where the cell is guaranteed by design to pass essentially through the center of the Gaussian beam, where the intensity is highest, any given pass in LR flow cytometry typically does not result in such a head-on interaction. Most times the laser beam sweeps by the cell askance, presenting its shoulder or tail to it. By analyzing the comb of multiple peaks resulting from successive scans, the envelope of such comb can be extracted and *its* peak height measured. This quantity is analogous to the "peak-and-hold" value of conventional flow cytometers.

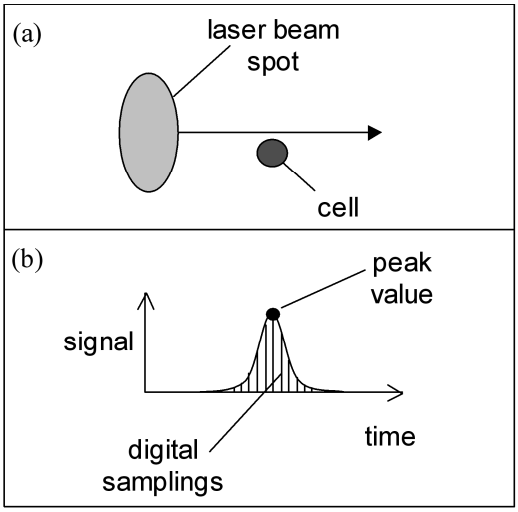

Fig. 3. First signal processing step. (a) Individual interaction of the laser beam with a cell. (b) The resulting pulse, fast digitizations, and stored pulse height.

[2] For a true Gaussian with zero or negligible offset, height and width are sufficient to uniquely determine the curve; area under the curve is sometimes extracted as well, and where the signals depart from true Gaussian shape, this third parameter can carry additional independent information that may be used to further separate cell populations from one another.

There are different approaches available in principle to carry out the analysis described above. Some are certainly suitable for offline processing; however, we were mainly interested in algorithms that could be performed in real time on the full stream of raw data being generated by the multiple detection channels. We therefore came up with a two-step process that quickly winnows down the amount of relevant data for further analysis without jeopardizing the quality of the measurement. In the first step, the data stream from each detector channel is digitized at high rates (about 100 MS/s), and peak locations and values (the comb's "teeth") are found within each separate raster scan and stored. Figures 3(a) and 3(b) illustrate this step. In the second step, the peaks so found are correlated across successive scans in order to build up the comb and its envelope; the envelope height is finally extracted for analysis. This second step is illustrated in Figs. 4(a)-(d).

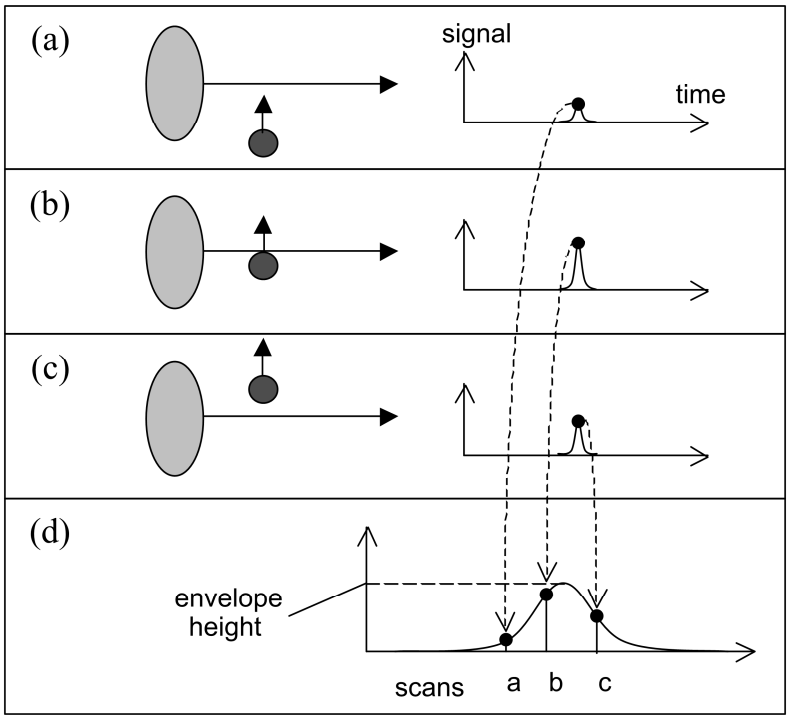

Fig. 4. Second signal processing step. (a-c) Three successive raster scans. On the left is a schematic representation of the laser-cell interaction; on the right the resulting signal waveform and varying pulse height. (d) The arrangement of successive pulse heights into a comb, determination of its envelope, and extraction of the envelope height for further analysis.

As indicated in Subsection 2.1, use of an AOD as in the design described here results in a variation of the transmitted laser intensity as the deflection angle is changed. This variation, if significant, requires correction in order to avoid unnecessary blunting of the precision of the system (the CV). In our system, such AOD compensation is carried out in the digital domain. In order to do so, the curve of transmission T vs. deflection angle θ is obtained by collecting digital samples of the ALL channel across the entire sweep range in the absence of scatterers. This curve is then used as a look-up table to correct every subsequent scan when assays are performed. We performed this operation using real scattering data from microspheres and offline MATLAB® processing, and the resulting CV was 3.1%—a very good outcome, given the number of elements that as of that time had not yet been optimized.

The choices of the various system parameters (such as, e.g., the digitization frequency, the sample stream flow rate and cross-sectional dimensions, etc.) reflect a complex balance of multiple constraints, biological, fluidic, electronic, and optical in nature. As an example, the rastering frequency was set to approximately 1 MHz, and the flow rate to about 3 m/s, in order to guarantee that any individual cell would be scanned multiple times by the sweeping laser beam; similar considerations resulted in analogous design choices throughout the system.

3. RESULTS AND DISCUSSION

We have implemented the concept described here using a combination of a prototype optical bench, off-the-shelf fast electronics, and modified reagents and hardware from a commercial hematology analyzer, Abbott Hematology's CELL-DYN Sapphire™. The AOD's compact form factor allowed its insertion into a standard 488-nm laser optical bench with few modifications. For the purpose of demonstrating the concept, we used a detector configuration yielding four scattering channels (ALL, IAS, PSS, and DSS—see Subsection 2.1). We additionally had one fluorescence channel available, which we put to service to detect either FL1 or FL3, depending on the assay. The results shown below reflect primarily one channel (IAS) as the most information-rich one for the purpose of this work. The detector electronics (preamplifier circuitry) was modified to keep up with the fast-changing signal profiles. An analog signal conditioning interface board was created to provide appropriate buffering for the digital board, as well as to accommodate future design needs. The digital signal processing module used was a commercial off-the-shelf, state-of-the-art system from Lyrtech[3] comprising eight 14-bit ADC channels clocked at a maximum of 104 MS/s, a Xilinx SX55 Virtex 4 Field-Programmable Gate Array (FPGA), onboard memory, and a PCI interface for communication to a host PC. The FPGA was coded in Verilog to implement the digital signal processing scheme described in Subsection 2.2. The signal processing module can be used in a number of different modes: (1) in simulation mode, virtual data created using a LabVIEW™ model of both the LR apparatus and the blood sample are fed to a complete simulation of the FPGA signal processing code, including timing; (2) in raw data mode, the ADCs collects real signals from all available detection channels at the full speed of up to 104 MS/s and stores the resulting raw digitized data in the onboard RAM for offline processing; (3) in hybrid mode, raw data collected as in mode 2 are fed to the FPGA simulator; (4) in rastering mode, the FPGA processes real data coming live from the ADCs in real time, batching the resulting cellular event information to a PC. Modes 1 and 3 were used to evolve and gain confidence in the signal processing algorithms during development; here we present mainly data collected using mode 2. For an upcoming report on real-time results using mode 4, see [5].

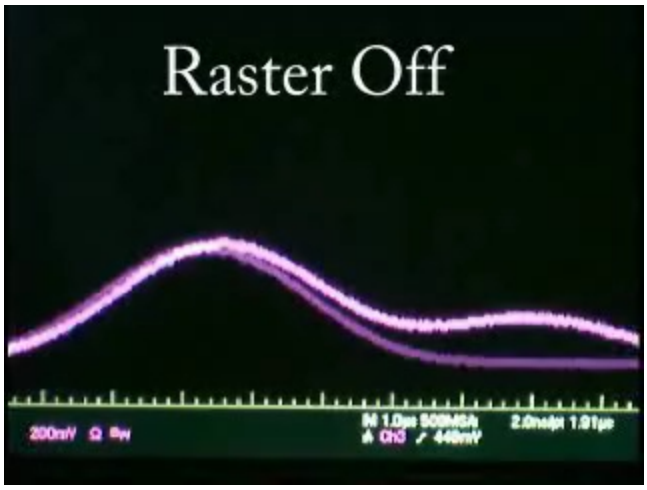

Video 1. Video showing oscilloscope traces of detector signals from microspheres. Rastering is initially turned off, then turned on while keeping the particle flow unchanged. http://dx.doi.org/10.1117/12.820799.1

The material in Video 1 (available as supporting multimedia material online) gives a graphical impression of the differences, both in terms of timescales and in terms of signal types, between conventional flow cytometry and LR flow cytometry. The video shows traces from the IAS detector channel captured in real time on an oscilloscope; rastering is turned off and on while the flow of monodisperse 7-μm-diameter polystyrene microspheres is maintained unchanged. The segment starts with rastering turned off: The broad pulses (one major division = 1 μs) trace the transit time of the particles across the stationary laser beam. When rastering is turned on, the broad pulses are replaced by combs of sharp spikes—each spike representing one pass of the laser beam over a microparticle. The combs are modulated by envelopes having the same shape and width as the broad pulses in the off state. This material demonstrates at a basic level the

[3] Lyrtech Inc., 4495 Wilfrid-Hamel, Quebec City, Quebec, Canada. www.lyrtech.com

validity of the LR concept, reproducing faithfully the very features predicted during concept formation and initial design—namely, cellular detection events represented by equidistant, well-defined sharp peaks under a Gaussian envelope. The sharpness of signals in LR highlights the need for proper design of detector electronics to avoid blurring of important features.

Figure 5 shows data from fresh human whole blood. Data from 488-nm excitation were acquired with the system scanning at 1 MHz and digitizing at 104 MS/s. A very short segment (20 μs) of the digitized output of a single detector channel (IAS) is shown, out of a data set comprising about 600 μs from three scattering channels and one fluorescence channel. The data were processed offline in MATLAB® and Excel™; the algorithms applied consisted of an AOD compensation step (analogous to the function coded in the FPGA) as well as of a baseline restoration step (a signal preprocessing function typically performed by analog circuitry in conventional flow cytometers)[8].

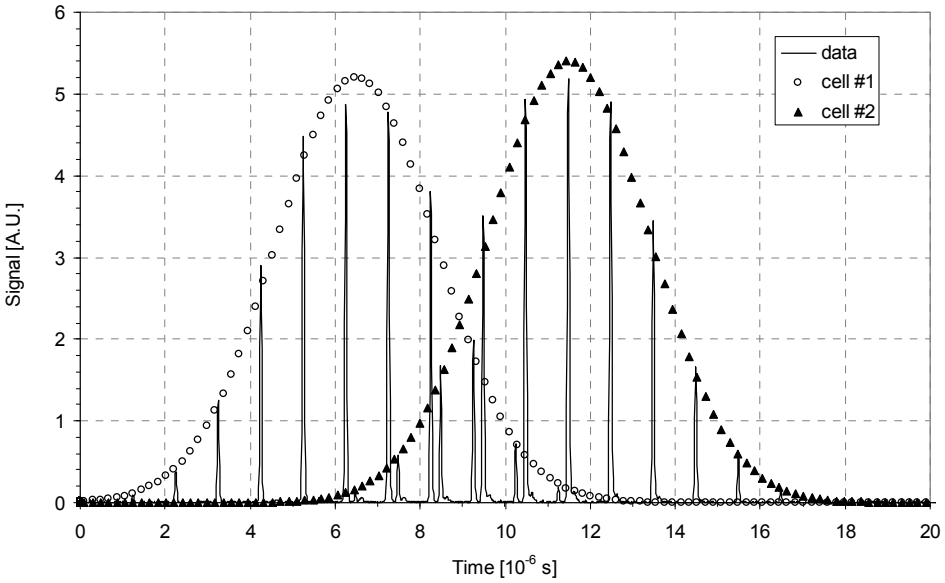

Fig. 5. LR data showing a "coincident" event being resolved. Two interlacing combs of LR peaks indicate the passage of two RBCs in close proximity. The Gaussian curves (open circles and solid triangles) are guides to the eye indicating the approximate envelope of each comb.

The segment was chosen because it illustrates the ability, with LR, to discern two closely spaced events—represented by the two interlacing combs of peaks with separate Gaussian envelopes. The two events in this figure were RBCs, separated laterally by about 50 μm and longitudinally (along the flow direction) by 5 scans—corresponding to 5 μs, and about 15 μm, at the raster frequency and flow rate used. Both of these two directions of resolution are important in terms of improving the system measurement rate, as they contribute in different ways to shrinking the effective detection volume. Simplifying, separation of individual spikes allows side-by-side cells to be distinguished; separation of Gaussian envelopes allows back-to-back cells to be distinguished. The overall result is to allow a greater cross-sectional sample stream, a higher concentration of cells, or a combination of the two, resulting in a sizable increase in the number of cells that can be identified per unit time.

What the data in Fig. 5 also show is the regularity of the signals in LR. Concerns about timing jitter, potentially causing misalignment of successive scans and making interpolation difficult, are put to rest by an analysis of peak locations such as those in this data set, which indicates that any jitter present is below one pixel width—approximately 10 ns, making it a non-issue for the purpose of this application. Equally importantly, the integrity of the signal (both in terms of jitter and in terms of peak sharpness) extends to the fluorescence detection channel. This means that fluorescence-based assays, whether using nucleic-acid dyes or conjugated monoclonal antibodies, can be implemented on a LR flow cytometer. The main difference in this case (apart from the signal-processing approach described above) is in excitation levels. Because the laser beam passes over a cell in a much shorter time than is typically the case in a conventional flow cytometer, the shorter excitation period needs to be compensated by a higher excitation photon flux in order to yield a comparable integrated emission. By design, a LR beam is already focused much more tightly than in conventional systems, bridging

much of the gap. The remaining difference (which is system-dependent and, for the system we analyzed, is estimated to be a factor of around 4) can be addressed in several ways. For assays far from the noise floor, a limited reduction in emission intensity may not be consequential and can simply be designed in. For more sensitive assays, there are three choices: increasing the laser power, increasing the amount of fluorophores ultimately binding to the cells of interest, or slowing down the raster speed. The third option forces a tradeoff with the goal of increasing the measurement rate and is not a first choice. We have experimented successfully with the other two and will be presenting results in upcoming works.

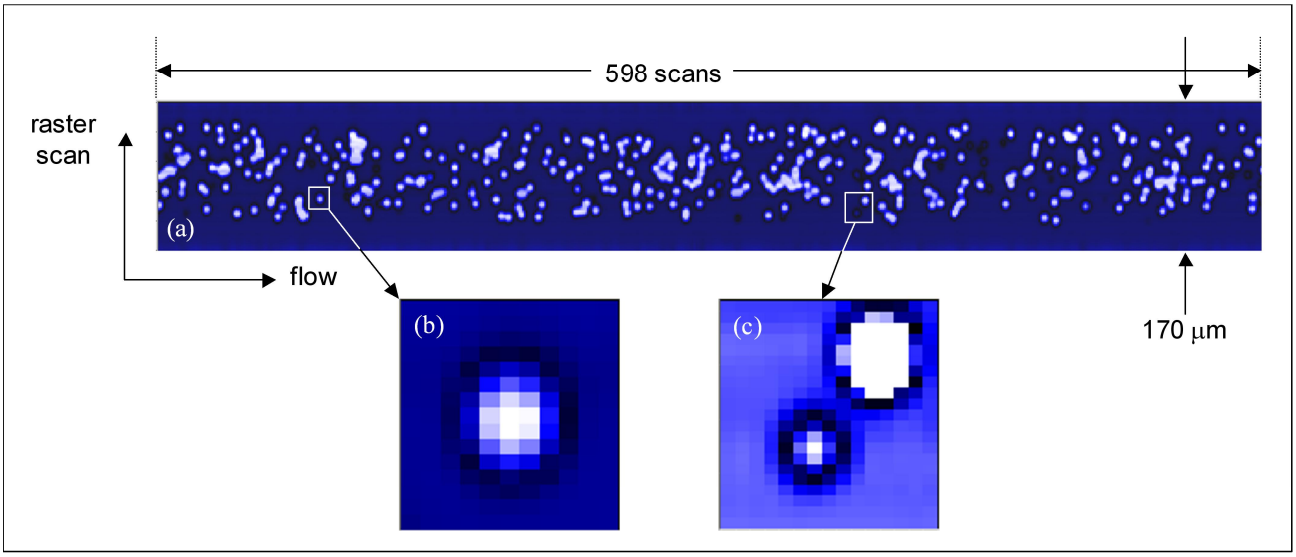

Fig. 6. LR data from a blood specimen. The data are arranged so that each pixel corresponds to a digitized sample from the IAS channel; each column comprises a single raster scan, about 170 μm from top to bottom. The color scale indicates signal strength, white being highest and black lowest; the scale varies from (a) to (c). (a) A 598-scan section of the data, corresponding to 0.6 ms of flow time. (b) A blow-up of an RBC event. (c) A blow-up of two neighboring events (RBC and platelet).

Figure 6 presents LR data from a fresh human blood sample assayed with 488-nm excitation. The data come from a mode-2 run on the LR system scanning at 1 MHz—real signals, digitized through the ADCs at 104 MS/s and stored in memory. AOD compensation and baseline restoration were not applied to this particular data set; raw pixel values are shown. Using MATLAB® and LabVIEW™ software, the data were arranged in such a way as to create a two-dimensional representation. The continuous data stream from one of the detector channels (IAS) was first cut up into individual sections (the columns in the figure), corresponding to single raster scans and spanning about 170 μm from top to bottom. A pixel in this representation corresponds to one digitization in the stream, with the color scale mapping signal height (black is lowest and white is highest). Each pixel corresponds to about 1.7 μm in the scan direction (vertical) and about 3 μm in the flow direction (horizontal). The scan-length sections were then lined up side by side, with one end representing the beginning of the scan and the other end its completion. In this way, a visual representation was created that corresponds to the stream of sample passing through the flowcell.

In Fig. 6(a), a 598-scan section of the data is shown, corresponding to 0.6 ms of flow time. About 360 cellular events can be counted. In terms of signal heights, two distinct populations emerge: a majority population of about 330 higher-intensity events (RBCs), and a much smaller population of about 30 lower-height events (platelets). To highlight the two types of events, two insets are shown with adjusted color scales: Fig. 6(b), a blow-up of an RBC event; and Fig. 6(c), a blow-up of two closely spaced events, an RBC and a smaller platelet. Because no post-processing was applied, the event peaks are surrounded by dips (darker pixels); this artifact is eliminated (as in Fig, 5) with proper baseline restoration. Note the clear differences between the platelet and RBC, not only in signal strength, but also in terms of width in both dimensions. While this two-dimensional representation does not constitute a true image (since it is a mapping of scattering information averaged, pixel by pixel, over the whole cell), IAS signals do have a significant correlation with size, and the observed event widths are consistent with the relative typical sizes of platelets and RBCs (diameters of 1-4 μm and 7-7.5 μm, respectively[9][10]), suitably convoluted with the laser beam widths (20 μm along the flow direction and 10 μm across it). This observation indicates that more information than simply signal height can be extracted from LR

data; for example, time-of-flight measurements of an interaction event, from each of the scans in the event and from each of the detection channels used, could provide independent sizing information supplementary to that obtained by forward scattering.

The significance of these results has several components. First of all, the sheer rate of cells that can be assayed is far in excess of the current state of the art. The cell measurement rate shown in Fig. 6(a) is on the order of 600,000 cells per second. State-of-the-art hematology analyzers are able to count cells at an approximate rate of up to 60,000 per second, but full identification and classification limits that rate to about 10,000 per second.[4] The data in Fig. 6 actually contain a nonnegligible number of RBC coincidences, something that can be, and typically is, addressed in the algorithm domain but that it is best to keep within low bounds. So, in practice, a less concentrated dilution would be used in order to mitigate the coincidence rate. We ran samples at a rate of approximately 300,000 cells per second with a significant improvement in coincidence events. Even if a further reduction in cell density (say, by a factor of 2) were necessary to drive coincidences to even lower levels, the margin of improvement compared to current technology would still be a factor of 2.5 for indiscriminate cell counting, and a factor 15 for accurate signal determination and cell classification. A second aspect of these results is that platelets and RBCs can be accurately distinguished using the LR approach. This was fully expected based on our experience and design parameters, but the data bear it out clearly. In an upcoming publication[5] we will additionally show how WBCs are likewise accurately captured by the system and distinguished from either RBCs or platelets.

4. CONCLUSIONS

The laser rastering (LR) flow cytometry concept, described here in its essential elements and corroborated by proof-of-concept data from prototype implementation, promises to deliver much greater cell measurement rates than are possible today. The advance is made possible by the introduction of a beam-scanning function, performed by an AOD, by adopting adequately fast digital-domain signal processing, and by performing data reduction based on peak analysis and scan-to-scan correlations. Our data confirm and even exceed design expectations, in terms of signal profiles, coincidence rejection, and cell measurement rates. The signals corresponding to RBCs and platelets in a blood assay were clearly distinguishable in the data. The next steps in this work, already in progress, aim to demonstrate the signal processing algorithms described here operating in real time on the digital module, and to demonstrate LR's ability to count and identify all major cellular classes in peripheral human blood (RBCs, platelets, and several subtypes of WBCs) at high measurement rates.

REFERENCES

[1] Vacca, G., Goldblatt, N. R., and Yee, M. W., "Method and apparatus for rapidly counting and identifying biological particles in a flow stream," US Patent Application No. 20080158561/A1 (2007).

[2] Vacca, G., *et al.*, "Laser rastering: a new high-speed approach to flow cytometry," ISAC XXIV International Congress, Budapest, Hungary, paper #5 (2008).

[3] Lui, W. W., *et al.*, "Digital signal processing scheme for laser rastering," ISAC XXIV International Congress, Budapest, Hungary, paper #394 (2008).

[4] Junnarkar, M. R., *et al.*, "Laser rastering: optics layout and experimental results," ISAC XXIV International Congress, Budapest, Hungary, paper #393 (2008).

[5] Vacca, G., *et al.*, Cytometry Part A (manuscript in preparation).

[6] Shapiro, H. M., [Practical Flow Cytometry], 4th ed., John Wiley & Sons, Hoboken, New Jersey, 19-20 (2003).

[7] de Grooth, B. G., Greve, J., and Terstappen, W. M. M., "Particle discriminator and method," US Patent No. 5017497 (1991).

[8] Shapiro, H. M., [Practical Flow Cytometry], 4th ed., John Wiley & Sons, Hoboken, New Jersey, 190-191 (2003).

[9] Anderson, S. C., and Poulsen, K. B., [Atlas of Hematology], Lippincott Williams & Wilkins, Baltimore, Maryland, 134 (2003).

[10] Anderson, S. C., and Poulsen, K. B., [Atlas of Hematology], Lippincott Williams & Wilkins, Baltimore, Maryland, 10 (2003).

[4] These numbers are obtained from an engineering analysis of samples run on Abbott Hematology's CELL-DYN Sapphire™ analyzer.